THE JOURNAL OF PHYSICAL CHEMISTRY B

ARTICLE

pubs.acs.org/JPCB

Dissecting the Energetics of Hydrophobic Hydration of Polypeptides

Silvina Matysiak,[†,§] Pablo G. Debenedetti,[‡] and Peter J. Rossky*[,†]

[†]Institute for Computational Engineering and Sciences and Department of Chemistry and Biochemistry, University of Texas at Austin, Austin, Texas, 78712 United States

[‡]Department of Chemical and Biological Engineering, Princeton University, Princeton, New Jersey, 08544 United States

[§]Fischell Department of Bioengineering, University of Maryland, College Park, Maryland, 20742 United States

ABSTRACT: The energetics of water proximal to apolar groups is analyzed from a statistical perspective in the realistic context of polypeptide hydration. Analysis of a series of molecular dynamics simulations of a 16-residue polypeptide in water reveals a correlation between hydrogen bond energy and local packing when there is overcoordination of the water molecules around hydrogen bonds. We show that the origin of the greater strength of hydrogen bonds in the hydrophobic hydration shell when compared to bulk water correlates with the depletion of water nearest neighbors around apolar moieties. The water molecules in the hydrophobic hydration shell sample the hydrogen bonding patterns present in comparable relatively low coordination regions of bulk water. We also find that for hydrophobic hydration shell water molecules the probability distribution of hydrogen bond energies is independent of the number of hydrogen bonds formed with other water molecules inside and outside the polypeptide hydration shell. This lack of correlation of hydrogen bond energy with hydrogen bond number leads to a remarkably accurate simplified statistical model for the energetics of hydrophobic hydration.

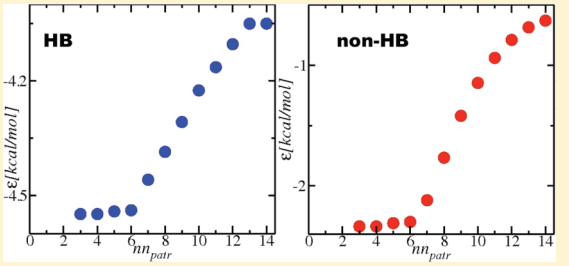

INTRODUCTION

The relationship between water as a solvent and protein behavior has been a very active topic of research for many decades.[1] It is generally accepted that hydration strongly influences the stability, dynamics, and function of proteins. Even though much has been learned about the unusual properties of water, there is still controversy regarding the importance of correlations between hydrogen bonds[2−4] and the details of hydrophobic hydration.[1,5] In particular, it has been speculated that correlations among hydrogen bonds might play an important role in determining the properties of water,[6−9] and thus understanding the existence of hydrogen bond correlations is of importance for obtaining a complete picture of a key element in protein structure, hydrophobic hydration phenomena.

The hydrophobic effect is manifested as a restructuring of the water solvent near an apolar moiety which is believed to be the cause of the sequestration of a protein's apolar residues in the core of the molecule, avoiding exposure to water. Each water molecule near an apolar moiety is strongly biased against sacrifice of any of its hydrogen bonds, leading inevitably to a significant orientational preference of water molecules at the surface of nonpolar residues.[10,11]

Several traditional views such as Frank's iceberg model[12] are still used within the scientific community to interpret experimental and computational studies.[1,5] According to this model, water molecules around hydrophobic groups form "ice-like" cages in which their hydrogen bonds are stronger than in bulk. However, recent computational studies have found that the hydrogen-bonded network seems to maintain its structure simply by orienting the O−H bonds tangentially to the solute surface.[1] The structure of the "icebergs" is not like the ordered structure observed in ice but rather resembles hydrogen-bond networks also found in bulk water. The icebergs are dynamically slowed but liquid water-like as far as structure is concerned.[13]

In particular, the source of the apparent greater "strength" of hydrogen bonds in the hydrophobic hydration shell around apolar moieties is still being debated.[1] Zichi et al.[10,11] showed that the strengthening, on average, of hydrogen bonds in the hydration shell is due to a reduction in the number of weaker, presumably strained, hydrogen bonds compared to the bulk. They concluded that what is modified is not the individual hydrogen bond strengths but rather a change of the population of hydrogen bonds.

The water molecules in the hydrophobic hydration shell are the ideal system to study the presence of hydrogen-bond correlations while removing bulk density effects from the analysis. Experimental evidence suggests a lack of energetic correlations between adjacent hydrogen bonds in liquid water. Walrafen[14] performed a Raman and IR spectral investigation of water structure and measured the intensity identified with broken and formed bonds over a wide temperature range. The dependence of the logarithm of the apparent equilibrium constant for bond breaking on $1/T$ gave a constant slope (see Figures 24 and 25 in ref 14). This result implies that the enthalpy of

Received: August 18, 2011
Revised: October 24, 2011
Published: October 31, 2011

breaking a bond does not change much when going from more highly hydrogen bonded states at low temperature to states with fewer hydrogen bonds at high temperature. If there was a significant energetic correlation between adjacent hydrogen bonds, one would anticipate a temperature dependence of the slope.

In principle, all-atom simulations can provide microscopic insight regarding such correlations. Different conclusions have been drawn from computational studies regarding the presence of correlations among hydrogen bonds. Raiteri et al. studied the dynamics of single and neighboring pairs of hydrogen bonds in bulk water[4] without further classifying the tagged bonds and concluded that the short time correlation between two coupled hydrogen bonds cannot be described assuming statistical independence. On the other hand, Luzar and Chandler studied single hydrogen bond dynamics by partitioning the trajectory according to the bonding environment[3] and concluded that the dynamics of hydrogen bonds is uncorrelated with specific bonding patterns near the tagged hydrogen bond. The two pictures do not appear consistent, and thus further simulation study of the intermolecular correlations of hydrogen bonds is warranted.

The goal of the present work is to obtain a clear picture of the energetics and the role of hydrogen bond correlations in these energetics both in bulk water and for water molecules belonging to the hydrophobic hydration shell of proteins. Rather than considering idealized solutes, such as apolar spheres, we carry out this study for a realistic model of a polypeptide. As one of the smallest peptides which exhibits many features of a full size protein, the C-terminal β-hairpin of protein G has been studied on both experimental and theoretical fronts[15,16] and represents an ideal system for dissecting the energetics of hydrophobic hydration in proteins.

We first focus on gaining a quantitative understanding of the energetic distributions of hydrogen bonds among water molecules in bulk and hydrophobic hydration shell environments. Since the thermal disorder of water molecules produces local density fluctuations around hydrogen bonds in bulk water, one focus will be understanding if and how the hydrogen bond energy is affected by these local density changes. By disentangling the energetic contributions (from hydrogen-bonds and non-hydrogen-bonded nearest-neighbors and non-nearest-neighbors) to the binding energy of a water molecule in the hydrophobic hydration shell of apolar residues of the β-hairpin, we investigate if there is correlation between these energetic contributions and how these correlate with the local solvent structure.

METHODS

The 16 residues (GEWTYDDATKTFTVTE) of the C-terminus of the immunoglobin binding protein G (Protein Data Bank ID code 2gb1)[16] have a β-hairpin topology and are chosen for this study. This 16-mer peptide contains four hydrophobic residues—Trp43, Tyr45, Phe52, and Val54—that form an extended and exposed surface in the folded state. The folded β-hairpin peptide structure is obtained by cutting these sixteen residues from the complete NMR structure and then acetylating and aminating the N-terminus and C-terminus, respectively.[15] The solvated system that we construct from this structure has 3774 water molecules and also three counterions (Na^+ ions) to neutralize the molecular system. The TIP3P model[17] is used for water, and the CHARMM force field[18] is used to model the polypeptide. All of the molecular dynamics simulations are carried out with NAMD.[19]

Since it is well established that there is a cooperative component contributing to hydrogen bond energetics in the condensed phase, associated with the role of polarizability, one might expect that there would be some quantitative difference in the energetics obtained with a polarizable or fully ab initio water model. Nevertheless, tests examining the structure and hydrogen bonding in water at hydrophobic interfaces using such models have found only minor differences compared to results obtained with models in the which molecular polarization is treated in an average way, such as that we use here.[20] Hence, we believe that the present analysis should be robust to such variations in the water model.

The structure of the fully solvated system is first locally minimized in potential energy using the conjugate gradient method. For the purpose of our analysis, the backbone of the peptide is subsequently fixed in space, but the side chains move freely. The fixed backbone of the polypeptide helps us to better understand the dependence of hydrogen-bond behavior on the surface topography since removing the mobility of the polypeptide backbone removes a potentially confounding fluctuation. The long-range electrostatic interactions with periodic boundary conditions are calculated by the particle-mesh Ewald method. A time step of 2 fs is used, and the RATTLE method is applied to keep the water rigid and the bond lengths fixed. The system is equilibrated for 100 ps in the NPT ensemble (at p = 1 atm and T = 298 K) reaching a constant density of 0.994 g/cm^3, and finally a 100 ps NVT simulation is performed before the production run. A 1.5 ns microcanonical simulation at an average temperature of 298 K is then performed. Every 20 fs, a configuration is saved for the analysis below. A simulation of bulk water is also performed, at the same conditions and using the same simulation protocol as the polypeptide in water to compare the properties of hydrophobic hydration with those of bulk water.

For the purpose of analysis, we need to define the environments of individual water molecules and the hydrogen bonding state of molecular pairs. We employ a widely used definition of solvation shells. The hydrophobic solvation shell is comprised of the water molecules in which the oxygen atom is closer to the hydrophobic C-atoms of the selected hydrophobic amino-acids than to any other solute atom,[21] while at the same time satisfying the constraint that the separation from the C-atoms is not greater than 4.0 Å. The C-atoms are conveniently classified by the atomic partial charge magnitude. It has been shown that depending on the charge magnitude, the C-atoms can behave as polar or nonpolar;[22] C-atoms with partial charge magnitudes up to 0.265 are considered nonpolar and atoms with larger magnitudes are considered polar.[22] With this classification, all of the carbon atoms of the selected hydrophobic residues in the present case are hydrophobic except the C-atom of the backbone. The total hydration shell of the polypeptide is defined as the water molecules in which the oxygen atom is closer than 4.0 Å to C-atoms and 2.8 Å to N and O atoms.[23] Of particular interest are the water molecules in the following defined environments: (O) the water molecule is in bulk, thus it is outside the polypeptide's hydration shell; (IB) the water molecule is inside the hydration shell of the hydrophobic C-atoms of TRP43, TYR45, PHE42, and VAL54; (I) the water molecule is inside the total hydration shell of the polypeptide so it includes the water molecules of the environment IB plus the hydration shell of polar atoms.

We define nearest-neighbor water molecules by including only water molecules with oxygen-atom separations within 3.5 Å (the range of a water first coordination shell). The number of nearest

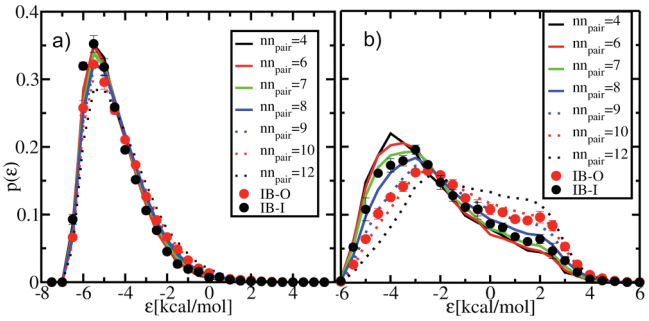

Figure 1. Comparison of interaction energies of nearest-neighbor waters in different environments. (a) The solid lines correspond to the probability distribution of hydrogen-bond energy for several values of the number of nearest neighbors around a pair of neighboring water molecules (nn_{pair}) for bulk water. The points correspond to the hydrogen-bond energy of hydrophobic hydration shell waters forming a bond with a water molecule in the polypeptide hydration shell (IB-I) and with a water molecule outside the hydration shell (IB-O). (b) The solid lines correspond to the probability distribution of nearest-neighbors non-H-bonded interaction energy for several values of nn_{pair} for bulk water. The points correspond to the nearest-neighbors non-H-bonded interaction energy for hydrophobic hydration shell waters in the IB-I and IB-O environments. The bars on data points for the probability distribution of interaction energies for pairs involving the hydration-shell indicate the energetic difference observed when comparing the total hydrophobic hydration shell around the selected atoms with the individual hydration shell of each of the hydrophobic residues.

neighbors around a pair of neighboring water molecules (nn_{pair}) is defined by the number of nearest neighbors around both molecules forming the pair without double counting and without counting either molecule in the nearest neighbor pair as one of these neighbors. For example, if both water molecules in the pair have tetrahedral coordination, $nn_{pair} = 6$; each molecule in the pair has three distinct nearest neighbors, excluding the paired molecule. In order to define when a hydrogen bond is formed, a commonly used geometric criterion is adopted. A water pair is hydrogen-bonded if the oxygen−oxygen distance is not greater than 3.5 Å and simultaneously the bonded O−H···O has a HOO angle that is not greater than 30° (estimated amplitude of librations that breaks hydrogen bonds[24]). The environment of a hydrogen bond is classified according to the two molecules forming the bond (e.g., IB-I, means that one water molecule is in the hydrophobic hydration shell and the other one belongs to the polypeptide hydration shell). We define the bonding state of a hydrophobic hydration shell water molecule according to the number of hydrogen bonds with other water molecules inside and outside the polypeptide hydration shell, which are denoted by N_{HB}(IB-I) and N_{HB}(IB-O), respectively.

RESULTS AND DISCUSSION

To relate the energetic behavior of hydration water molecules around hydrophobic moieties to a microscopic picture, we first compare the properties of bulk water with properties of hydrophobic hydration shell water molecules. We characterize changes in the dimer energy (interaction energy of nearest-neighbor water molecules) of H-bonded (hydrogen bonded) and non-H-bonded pairs as a function of nn_{pair} for bulk water molecules and for water molecules in the (IB-I) and (IB-O) environments as shown in Figure 1.

As depicted in Figure 1a, the distribution of hydrogen-bond energies (defined as the probability of finding such a pair of molecules interacting with a potential energy ε) shows an increase in the likelihood of weaker hydrogen bonds when there is over-coordination compared to an ideal tetrahedral case ($nn_{pair} > 6$) around the pair of interacting water molecules. This effect is much more pronounced for nearest-neighbor molecules that are non-H-bonded (see Figure 1b). Moreover, the energy at which the distribution is maximum is independent of nn_{pair} for hydrogen-bonded pairs, whereas for the nearest-neighbor water molecules that are non-H-bonded, it shifts toward higher energies, as expected. Therefore, there is a reduction of non-H-bonded pairs with favorable interaction energies as nn_{pair} is increased, whereas for hydrogen-bonded pairs there is no significant reduction of stronger hydrogen bonds. To further emphasize the behavior of the energetic distributions of Figure 1 for bulk water, we present in Figure 2 the mean energy of the distributions of Figue 1 as a function of nn_{pair}. We find that for bulk water there is a strong correlation between nn_{pair} and the interaction energy of nearest-neighbor water molecules for hydrogen-bonded and for non-H-bonded pairs when $nn_{pair} > 6$, with a much larger impact for the latter pairs.

To correctly assess the differences and similarities of the distributions of bulk water of Figure 1 compared to the hydration shell, the residual is computed by subtracting from the distributions for bulk water those of the hydration shell. As shown in Figure 3, the energetic distribution functions for hydrogen-bonded pairs in the bulk that are not overcrowded ($nn_{pair} \leq 6$) have the smallest deviations from the energetic distribution of hydration water molecules in the IB-I environment. On the other hand, the IB-O hydrogen-bonded energetic distribution has the smallest residuals from the bulk distributions when there is a fifth neighbor around each water molecule ($nn_{pair} = 8$). At least qualitatively, then, the water molecules in the IB-I environment sample the hydrogen bonding patterns present in not over-crowded regions of bulk water ($nn_{pair} \leq 6$), whereas the water molecules in the IB-O environment sample the hydrogen bonding patterns present in bulk water when there is an excess neighbor around each water molecule ($nn_{pair} = 8$).

Figure 2c shows that there is a shift in the probability distribution of observing a certain nn_{pair} depending on the water environment and that the IB-I distribution is clearly more narrow than the bulk. Furthermore, non-H-bonded pairs are more crowded than hydrogen-bonded ones. For IB-O non-H-bonded pairs, the energetic distribution has the smallest residual from the bulk distributions when nn_{pair} is between 9 and 10. The fact that non-H-bonded pairs have more nearest neighbors than hydrogen-bond pairs indicates that the incorporation of extra water neighbors and crowding leads to possible loss of hydrogen bonds by distortion. This agrees with the observation of Smith et al. that overcoordination is common among distorted hydrogen bonds.[25]

By analyzing the energetic properties of hydrogen bonds involving water molecules proximal to the exposed hydrophobic residues, we can separate the effects on hydrogen bond strength due to the bonding state of the molecules from those resulting from local density. Water binding energies (defined as the sum of interaction energies considering only pairs of water molecules that lie within a cutoff distance of 8 Å) are very sensitive to the local environment and thus reflect the relationship between energetics and local properties. By disentangling the different energetic contributions to the binding energy of a hydration water molecule, we can investigate if there is a correlation

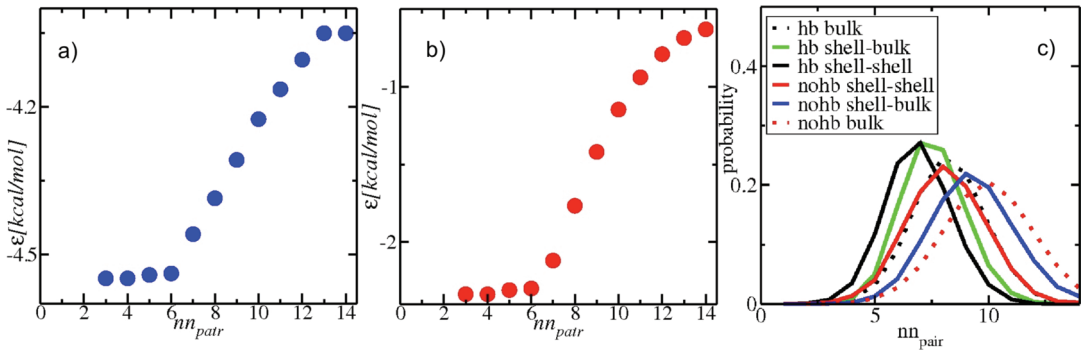

Figure 2. (a and b) Comparison of the dimer energy (kcal/mol) for nearest-neighbor water molecules as a function of the number of nearest-neighbors around the pair. Figure a corresponds for the pairs that are hydrogen-bonded, and Figure b to the ones that are not. Each dot corresponds to the mean value obtained from the distribution of interaction energies of nearest-neighbor bulk water molecules from Figure 1. (c) The probability distribution of observing two nearest-neighbor waters with nn_{pair} for different environments.

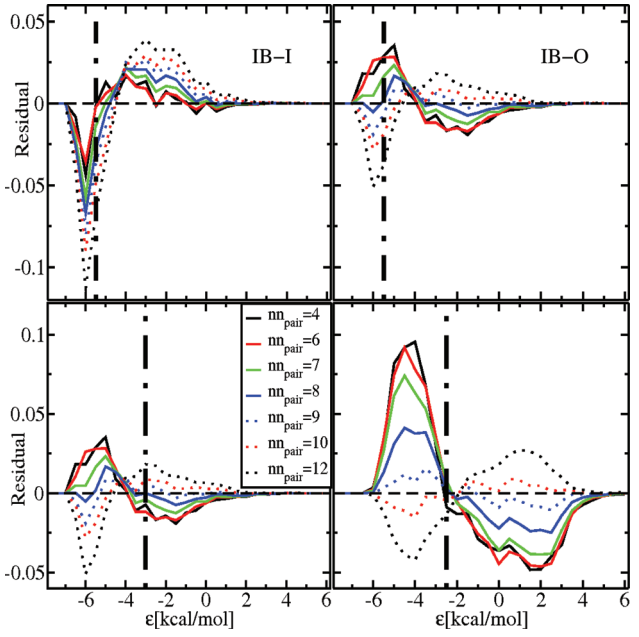

Figure 3. Comparison of the residual obtained from the distribution of interaction energies from IB-I (left column, hydrophobic hydration shell-polypeptide hydration shell) and IB-O (right column, hydrophobic hydration shell-bulk) pairs compared to the energetic bulk distribution as a function of the number of nearest neighbors around a pair of neighboring water molecules (nn_{pair}). The upper panels are for hydrogen-bonded energies, and the bottom are for non-H-bonded pairs. The vertical dashed line in the plots marks the position where the distributions for IB-I and IB-O are each maximum.

between these distributions and how each energetic contribution from hydrogen bonds, non-H-bonded pairs, and non-nearest-neighbors pairs (pairs of water molecules that are within 8 Å and are not nearest-neighbors) correlates with the local properties of the tagged water molecule.

In what follows, we present the results for bonding states labeled by the number of H-bonds of the two possible types (N_{HB}(IB-I) and N_{HB}(IB-O)) for three states and two residues that are representative: (1,1) (2,1), and (2,2) around residue TYR and PHE; similar results are obtained for other bonding states and hydrophobic residues. These states have a probability of observance of 19.64%, 14.25%, and 5.85%, respectively.

The total "hydrogen bond energy" $E_{HB}(N_{HB}(\text{IB-I}),N_{HB}(\text{IB-O}))$ of a tagged water molecule with N_{HB}(IB-I) hydrogen bonds within the hydration shell and N_{HB}(IB-O) hydrogen bonds with water molecules outside the hydration shell is just the sum of the interaction energy with its nearest neighbors that are hydrogen bonded in each environment. For statistically uncorrelated events, the probability $P(E_{HB}(N_{HB}(\text{IB-I}),N_{HB}(\text{IB-O})))$[29] should be completely determined by the convolution of unimolecular probabilities as follows:

$$P(E_{HB}(N_{HB}(IB\text{-}I),N_{HB}(IB\text{-}O))) = P(E_{HB}(N_{HB}(IB\text{-}I),0)) \otimes P(E_{HB}(0,N_{HB}(IB\text{-}O))) \quad (1)$$

with

$$P(E_{HB}(N_{HB}(IB\text{-}I),0)) = P(E_{HB}(1,0))\ldots \otimes P(E_{HB}(1,0)) \quad (2)$$

$$P(E_{HB}(0,N_{HB}(IB\text{-}O))) = P(E_{HB}(0,1))\ldots \otimes P(E_{HB}(0,1)) \quad (3)$$

where $P(E_{HB}(1,0))$ and $P(E_{HB}(0,1))$ appear in eqs 2 and eq 3 N_{HB}(IB-I) and N_{HB}(IB-O) times, respectively.[30] Figure 4 shows the agreement between the probability distribution $P(E_{HB}(N_{HB}(\text{IB-I}),N_{HB}(\text{IB-O})))$ for the hydration shell of TYR and PHE and the result of the application of eq 1. This result clearly implies that the energy of a hydrogen-bond in each environment (IB-I or IB-O) is essentially uncorrelated (within the noise of the simulation) with the number of hydrogen bonds formed by water molecules in the hydration shell.

The contribution from non-H-bonded nearest-neighbors to the binding energy ($E_{nn\text{-}nohb}$) is defined as the sum of interaction energies considering only pairs of water molecules that are non-H-bonded and lie within a cutoff distance of 3.5 Å to a hydration shell water molecule. The contribution from non-nearest-neighbors (E_{nnn}) is defined as the sum of interaction energies considering only pairs of water molecules that lie within 8 Å and are not nearest-neighbors to a hydration shell water molecule.

To test the hypothesis that $E_{nn\text{-}nohb}$ and E_{nnn} correlate with the local environment of the tagged water molecule, $E_{nn\text{-}nohb}$ and E_{nnn} are classified according to the number of hydrogen bonds of the tagged water molecule. We see from Figure 5a that the

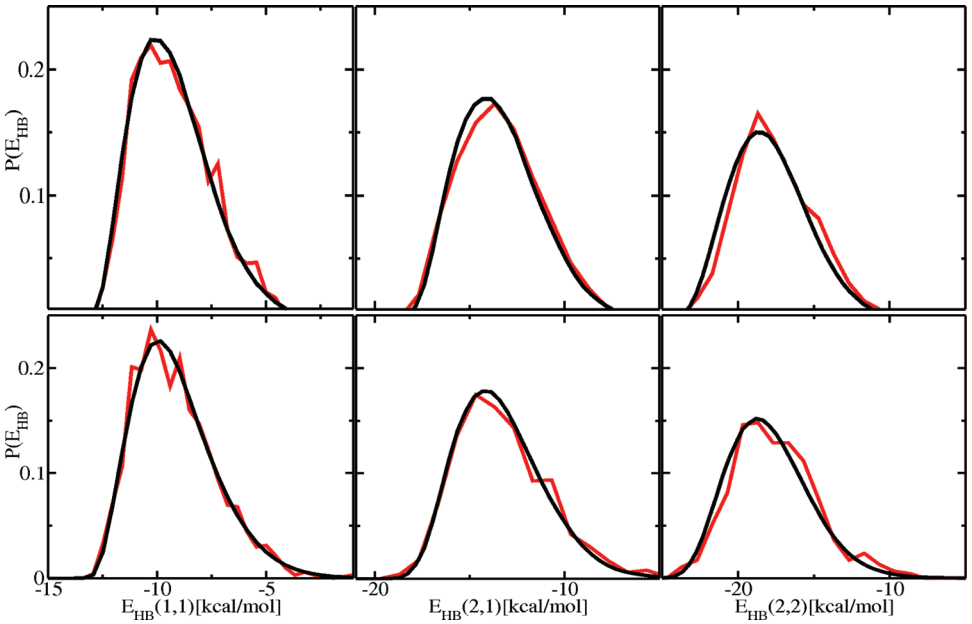

Figure 4. Hydrogen-bond contribution to the binding energy. The red curve is the probability distribution of the hydrogen-bond contribution to the binding energy E_{hb} of a tagged hydration water molecule in different bonding states. The black curve is the result of applying equation eq 1. The upper panels correspond to waters in the hydrophobic hydration shell of PHE, whereas the lower ones correspond to TYR.

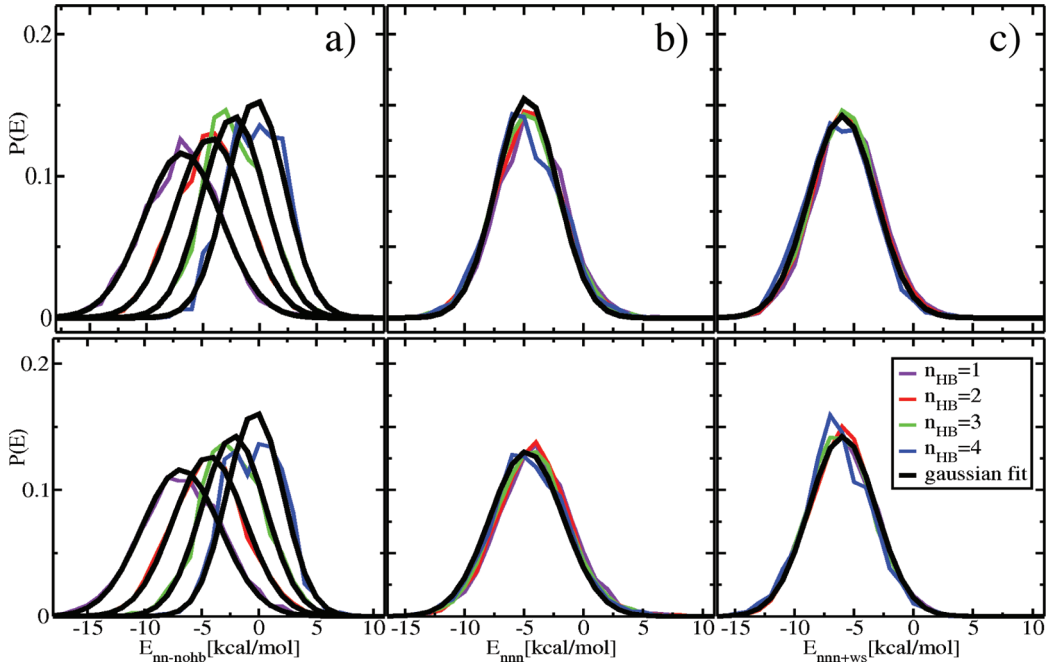

Figure 5. (a) Probability distribution of the contribution from non-H-bonded nearest-neighbors to the binding energy $E_{nn\text{-}nohb}$ of a tagged water molecule for several values of the total number of hydrogen-bonds in which the tagged molecule participates. (b) Probability distribution of the contribution from water−water non-nearest-neighbors to the binding energy E_{nnn} of a tagged water molecule for several values of the total number of hydrogen-bonds in which the tagged molecule participates. (c) Probability distribution of the contribution from non-nearest-neighbors (including water−protein and water−counterion interactions) to the binding energy E_{nnn} of a tagged water molecule for several values of the total number of hydrogen-bonds in which the tagged molecule participates. The upper panels correspond to the hydration shell of PHE, and the bottom panels correspond to TYR.

probability distribution of $E_{nn\text{-}nohb}$ ($P(E_{nn\text{-}nohb}(N_{HB}))$) can be well fitted to a progression of Gaussian distributions that only depend on N_{HB} with mean values $\nu = 2.15N_{HB} - 8.95$ and widths $\sigma = -0.32N_{HB} + 3.75$. Furthermore, the energetic contribution to the binding energy from non-nearest-neighbors, as shown in Figure 5, ($P(E_{nnn}(N_{HB}))$) does not depend on proximal water molecules; it collapses into a single Gaussian distribution independent of the number of hydrogen bonds that are formed for

dx.doi.org/10.1021/jp2079633 |J. Phys. Chem. B 2011, 115, 14859–14865

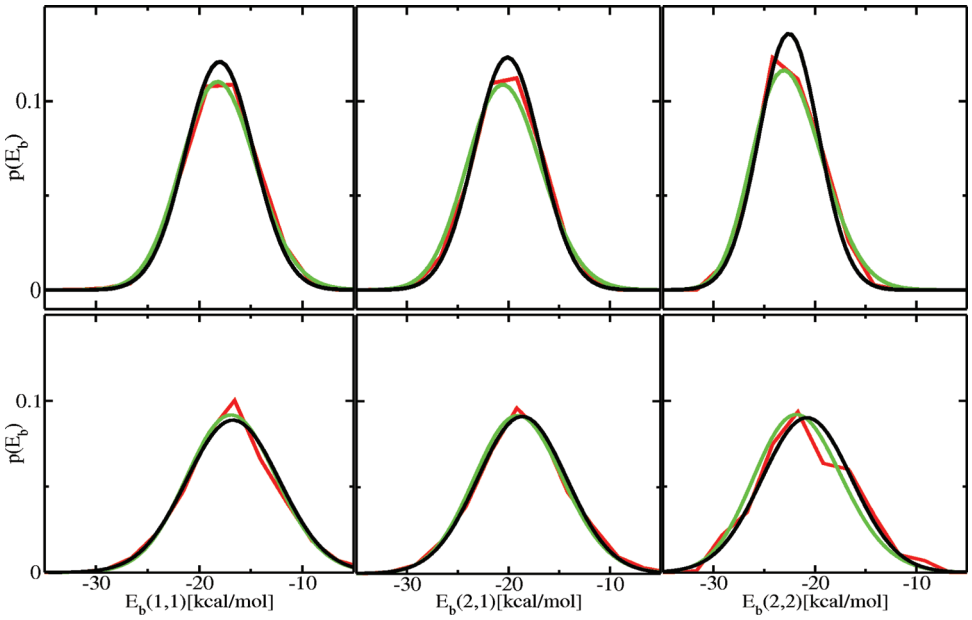

Figure 6. Probability distribution of binding energies (considering only water−water interactions) for the hydration shell of PHE (upper panels) and TYR (bottom panels) in different bonding states. The red curve corresponds to the simulation data, whereas the green curve is the result of applying eq 4. The black curve is a Gaussian fit of the data.

each hydration shell water molecule. However, there is some evident dependence on the residue identity, which is likely due to the proximity of charged amino-acids[26,27] (similar results are obtained for VAL and TRP). If the energetic contribution that comes from water−protein and water−counterion is added to the non-nearest-neighbor energy ($E_{nnn+ws} = E_{nnn} + E_{ws}$), then the probability distribution $P(E_{nnn+ws}(N_{HB}))$ shown in Figure 5c collapses remarkably into a single Gaussian distribution (mean $\mu = -5.97$ kcal/mol and width $\sigma = 2.81$ kcal/mol) independent of the residue.

Thus, we conclude that, to a quite good degree of accuracy, the binding energy of a water molecule (E_b) that comes from water−water interactions can be statistically expressed as

$$P(E_b(N_{HB}(IB\text{-}I), N_{HB}(IB\text{-}O)) = P(E_{HB}(N_{HB}(IB\text{-}I), N_{HB}(IB\text{-}O))) \otimes P(E^*(N_{HB})) \quad (4)$$

where

$$P(E^*(N_{HB})) = P(E_{nn\text{-}nohb}(N_{HB})) \otimes P(E_{nnn}) \quad (5)$$

is the probability distribution of the energetic contribution from non-H-bond water pairs to the binding energy. Figure 6 shows the agreement between the probability distributions obtained by applying the simple statistics expressed by eq 4 (green curve) and the probability distribution of binding energies, considering only water−water interactions, obtained from simulation data $P(E_b)$ (red curve), as well as a Gaussian fit to the simulated area.

The effect of polar groups and ions nearby to the studied hydrophobic hydration shell becomes clear from a comparison between average binding energies. The average binding energy E_b (resulting from water−water interactions) and the total binding energy E_{tb} (considering also the interaction water−protein and water−counterion), of proximal water molecules around the apolar atoms of the hydrophobic amino-acids Trp43, Tyr45, Phe52, and Val54 are shown in Table 1. When the water binding energy is computed also considering the water−protein and water-counterion interactions, the total binding energies of the hydration water molecules are similar to the bulk water binding energy (−19.8 ± 0.1 kcal/mol). The biggest deviation between the bulk binding energy and the binding energies of tagged water molecules considering only water−water interactions is for the hydration shell of TYR and TRP that are next to the charged amino-acids ASP and GLU, respectively.

Table 1. Water Binding Energies for Water in the Hydrophobic Hydration Shells of Alternative Residues, Including Only Water−Water Interactions (E_b) and also Including Water with Protein and Counterions (E_{tb})

residue	E_b (kcal/mol)	E_{tb} (kcal/mol)
PHE	−18.77 ± 0.1	−19.82 ± 0.1
TRP	−18.42 ± 0.1	−19.78 ± 0.1
VAL	−19.21 ± 0.1	−20.03 ± 0.2
TYR	−17.64 ± 0.2	−19.91 ± 0.2

CONCLUDING REMARKS

In order to obtain a microscopic picture of the statistics describing the energetics for hydrophobic hydration water molecules, we have studied the results of a simulation of water around the hydrophobic residues of a 16 residue hairpin structure. We have compared the changes in dimer energy in bulk water as a function of the local neighbor environment of the molecular pair with the dimer energy for water molecules pairs completely within the hydration shell of hydrophobic residues and those with one bonding partner outside this hydration shell. We have found that overcoordination around a pair of nearest-neighbor water molecules has a major influence on the strength of hydrogen bonds, which indicates a strong correlation of hydrogen-bond energy with local packing. Water can be viewed as a random three-dimensional network of hydrogen bonds where the local

environment around a hydrogen bond has a fluctuating number of nearest neighbors. The picture that emerges from our work is that the hydrophobic hydration of polypeptides originates from the fact that the polypeptide prevents the water molecules in the hydration shell from being approached by extra water molecules that would lead to overcrowding (and thus cause distortions among nearest-neighbor water molecules). The hydrophobic hydration water molecules are found to statistically mimic already existing hydrogen-bond patterns of bulk water that are present in noncrowded regions.[10,11] These statistical energetic results can be used to build simplified models, such as lattice models of proteins in explicit water to investigate protein folding and stability, and this will be the subject of a forthcoming publication.

For the purpose of understanding the presence of correlations of the different energetic contributions to the binding energy with the local environment, we have performed a statistical analysis of the different energetic contributions as a function of the number of hydrogen bonds formed by a hydrophobic hydration water molecule. We have found that the energy of a hydrogen bond is essentially uncorrelated with the number of hydrogen bonds around a specified water molecule in the hydration shell. This finding is in agreement with the inference made from experimental results by Walrafen[14] that shows that the enthalpy of breaking a bond does not change much going from a highly hydrogen bonded system at low temperatures to a system with fewer hydrogen bonds at high temperatures. The fact that the energy of a hydrogen bond is uncorrelated with the number of hydrogen bonds in the hydration shell is also in agreement with the lack of correlation between the dynamics of a hydrogen bond with its neighboring bonds at a fixed environment near the bond, as observed by Luzar et al.[2,3] The contribution to the binding energy from nearest-neighbors that are non-H-bonded is found to be dependent in a simple way on the bonding state of the tagged molecule, whereas the non-nearest-neighbor contribution is found to be independent of the water molecule's bonding state, and thus can be viewed as a background energy. Cooperativity in water might be a direct consequence of the strong energetic dependence of hydrogen bonds on the number of nearest neighbors when there is overcoordination. In addition, the large energy fluctuations evident in simulation of liquid water[28] can also be rationalized by the strong correlation of hydrogen-bond energy with local packing. Future work focusing on characterizing the energetics of hydrophobic hydration as a function of temperature and pressure is of considerable interest.

AUTHOR INFORMATION

Corresponding Author

*E-mail: rossky@mail.utexas.edu.

ACKNOWLEDGMENT

We are indebted to Dr. Lauren Kapcha for her insightful comments on an earlier version of this paper. P.G.D. and P.J.R. gratefully acknowledge the support of the National Science Foundation [Collaborative Research Grants CHE0908265 (P.G.D.) and CHE0910615 (P.J.R.)], and the R.A. Welch Foundation (F0019 (P.J.R.)). We are also grateful to the Texas Advanced Computing Center (TACC) at the University of Texas for high performance computing resources.

REFERENCES

(1) Ball, P. *Chem Rev* **2008**, *106*, 74–108.
(2) Luzar, A. *Chem. Phys.* **2000**, *258*, 267–276.
(3) Luzar, A.; Chandler, D. *Phys. Rev. Lett.* **1996**, *76*, 928–931.
(4) Raiteri, P.; Laio, A.; Parrinello, M. *Phys. Rev. Lett.* **2004**, *93*, 087801−1–087801−4.
(5) Blokzijl, W.; Engberts, J. B. F. N. *Angew. Chem., Int. Ed. Engl.* **1993**, *32*, 1545–1579.
(6) Green, J. L.; Lacey, A. R.; Sceats, M. G. *J. Phys. Chem.* **1986**, *90*, 3958–3964.
(7) Sciortino, F.; Fornili, S. L. *J. Chem. Phys.* **1989**, *90*, 2786.
(8) Stokely, K.; Mazza, M. G.; Stanley, H. E.; Franzese, G. *Proc. Natl. Acad. Sci. U.S.A.* **2010**, *107*, 1301–1306.
(9) Matsumoto, M.; Ohmine, I. *J. Chem. Phys.* **1995**, *104*, 2705–2712.
(10) Zichi, D. A.; Rossky, P. J. *J. Chem. Phys.* **1985**, *83*, 797–808.
(11) Rossky, P. J.; Zichi, D. A. *Faraday Symp. Chem. Soc.* **1982**, *17*, 69–78.
(12) Frank, H. S.; Evans, M. W. *J. Chem. Phys.* **1945**, *13*, 507–532.
(13) Rezus, Y. L. A.; Bakker, H. J. *Phys. Rev. Lett.* **2007**, *99*, 148301.
(14) Franks, F., Ed. *Water: A Comprehensive Treatise*; Plenum: New York, 1972; Vol. 1, p 205.
(15) Zhou, R.; Berne, B. J.; Germain, R. *Proc. Natl. Acad. Sci. U.S.A.* **2001**, *98*, 14931–14936.
(16) Blanco, F. J.; Rivas, G.; Serrano, L. *Nat. Struct. Biol.* **1994**, *1*, 584–649.
(17) Jorgensen, W. L.; Chandrasekhar, J.; Madura, J. D.; Impey, R. W.; Klein, M. L. *J. Chem. Phys.* **1983**, *79*, 926–936.
(18) Mackerell, A. D., Jr.; Feig, M.; Brooks, C. L., III *J. Comput. Chem.* **2004**, *25*, 1400–1415.
(19) Kale, L.; Skeel, R.; Bhandakar, M.; Brunner, R.; Gursoy, R.; Krawetz, N.; Phillips, J.; Shinozaki, A.; Varadarajan, K.; Schulten, K. *J. Comput. Phys.* **1999**, *151*, 283–312.
(20) Bauer, B. A.; Patel, S. *J. Phys. Chem. B* **2010**, *114*, 8107–8117.
(21) Methrotra, P. K.; Beveridge, D. L. *J. Am. Chem. Soc.* **1980**, *102*, 4287–4294.
(22) Carey, C.; Cheng, Y.; Rossky, P. *J. Chem. Phys.* **2000**, *258*, 415–425.
(23) Makarov, V. A.; Andrews, B. K.; Pettitt, B. M. *Biopolymers* **1998**, *45*, 469–478.
(24) Teixeira, J.; Bellissent-Funel, M. *J. Phys.: Condens. Matter* **1990**, *2*, SA105.
(25) Smith, J. D.; Cappa, C. D.; Wilson, K. R.; Cohen, R. C.; Geissler, P. L. *Proc. Natl. Acad. Sci. U.S.A.* **2005**, *102*, 14171–14174.
(26) Cheng, Y.; Rossky, P. J. *Nature* **1998**, *392*, 696–699.
(27) Cheng, Y.; Sheu, P. J.; Rossky, W. *Biophys. J.* **1999**, *76*, 1734–1743.
(28) Ohmine, I.; Tanaka, H. *Chem. Rev.* **1993**, *93*, 2545–2566.
(29) Where the probability density distribution of the sum of two independent random variables is the convolution of their density distributions: $(f \otimes g)(u) = \int_{-\infty}^{\infty} f(x)\, g(u - x)\, dx$ where $u = x + y$, x and y are random variables.
(30) The distribution of interaction energies of hydrogen-bonded pairs in the IB-I and IB-O environment collapses remarkably to a single distribution independently of the bonding state of the tagged water molecule, as seen in Figure 1a.